View metadata, citation and similar papers at core.ac.uk
brought to you by CORE
provided by PUblication MAnagement

Published in Microelectronics Journal 39, (12), 1594-1599, (2008) © 2009 Elsevier B.V. All rights reserved. DOI 10.1016/j.mejo.2008.02.005

Experimental characterization and numerical analysis of the 4H-SiC p-i-n diodes static and transient behaviour

Fortunato Pezzimenti[1], Francesco G. Della Corte[1], Roberta Nipoti[2]

[1]DIMET- Faculty of Engineering, Mediterranea University of Reggio Calabria
Via Graziella- Feo di Vito 89100 Reggio Calabria, Italy.
Telephone +390965875274, Fax +390965875463
fortunato.pezzimenti@unirc.it, francesco.dellacorte@unirc.it

[2]Institute of Microelectronics and Microsystems - CNR
Via Gobetti 101, 40129 Bologna, Italy
nipoti@bo.imm.cnr.it

Abstract

Steady-state and turn-off switching characteristics of Aluminium implanted 4H-SiC p-i-n diodes designed for high current density operation, are investigated experimentally and by mean of numerical simulations in the 298-523 K temperature range. The diodes present circular structure with a diameter of 350 μm and employ an anode region with an Aluminium depth profile peaking at 6×10^{19} cm^{-3} at the surface. The profile edge and the junction depth are located at 0.2 μm and 1.35 μm respectively. At room temperature the measured forward current density is close to 370 A/cm^2 at 5 V with an ideality factor always lower than 2 before high current injection or device series resistance became dominant. The transient analysis reveals a strong potential of this diodes for use in high speed, high power applications, especially at high temperature, with a very low turn-off recovery time (< 80 ns) in the whole range of test conditions. The simulated results match the experimental data, showing that the switching performance is mainly due to the poor minority charge carrier lifetime estimated to be 15 ns for these implanted devices.

Keywords: Silicon carbide; 4H-SiC p-i-n diode; *J-V* characteristic; Fast switching; High temperature; Carrier lifetime.

1. Introduction

Silicon carbide (SiC) has been identified as a wide bandgap material with the potential to offers great performance improvements in electronics, meeting requirements like higher breakdown voltages, thermal conductivity, switching frequencies, and efficiency [1, 2]. SiC based devices are more and more investigated for high-power, high-temperature, high-frequency and high-voltage switching applications [3-7]. For instance, short drift regions can be utilized without reducing the blocking voltage thanks to its extremely high breakdown electric field (a factor of 10 higher than in Si). This leads to a smaller on-state voltage drop and also a reduction of the device switching losses related to the decreased amount of carriers that must be swept away after blocking. Moreover, self-heating due to higher power densities is less critical and the device operation temperature is practically limited by external influences such as contacts and packaging issues.

SiC occurs in many different crystal structures and today the main polytype produced is the 4H considering its wider bandgap energy, that can be as wide as 3.26 eV, and a superior carrier mobility particularly suited for vertical devices realizations. Of course, the pace of progress in SiC device research is set by the availability of high purity and defect free large area epi-layers and by the continuous technological enhancements in the fabrication processes [8-10]. By the way, two of the most important issues are the control of impurity energy levels and the activation of ion implanted impurities, taking into account that the energy levels of dopants in SiC are much deeper than in Si and therefore these are not fully ionised at room temperature [11-13]. It is well know that Al (substitutional of Si site) and N (substitutional of C site) are the most common acceptor and donor impurities for SiC respectively, whereas ion implantation is the most feasible technique for the selective doping, since the diffusion coefficients of dopants are generally so low that thermal diffusion is rather difficult at reasonable temperatures. However, an appropriate post-implantation annealing, for the electrical activation of dopants and for recovering the crystalline structure, is required even when an ion implantation at high temperature is performed [11, 14]. The annealing conditions are crucial to obtain desired device electrical properties, independently if a planar or mesa semiconductor technology is performed. In fact, at the annealing temperatures the SiC morphology can seriously degrade, primarily by loss of Si atoms from the surface, with small SiC regions that no longer have the desirable crystal structure [8, 15].

In addition to the process technological progress, in the past recent years, numerical device modelling and simulations have gained increasing relevance for the analysis and optimization of electronic applications based on unconventional semiconductor like SiC. These tools in fact, not only help achieving an increased understanding of the device operation modes, but also, by comparing simulated and measured characteristics within a wide range of operation conditions, provide the ability to predict electrical behaviours and material parameters effects. In this paper, the commercial finite element device simulator ATLAS [16] was used to study the turn-off switching characteristics of Al implanted 4H-SiC p-i-n diodes at different temperatures. The tool supports the 4H polytype with a specific set of physical models already calibrated by comparison to experimental results in a previous work on the same sample diodes [17].

2. Device structure

A commercially available <0001> 8° off-axis n/n^+ 4H-SiC epitaxial wafer, manufactured by CREE Research Inc., was used for the fabrication of Al implanted p-i-n diodes with completely planar technology. The device structure was circular with a diameter of 350 μm and an active area close to 10^5 μm^2. The starting n^+ substrate has a doping concentration of 5×10^{19} cm^{-3}, whereas the n-type epitaxial layer was 5 μm thick with a donor doping of 3×10^{15} cm^{-3}. The implanted anode region showed a plateau aluminium concentration of 6×10^{19} cm^{-3} located at the surface, with a profile edge located at 0.2 μm and a profile tail crossing the epilayer doping at 1.35 μm, as verified by Secondary Ion Mass Spectrometry (SIMS) measurements. The chemical profile of the aluminium implanted doping concentration is shown in Fig. 1, where also the n-type epilayer concentration is pointed out. Further details about the diode fabrication process, post-implantation annealing conditions and ohmic contacts deposition, were described elsewhere [18].

For the electrical characterization, several devices placed on the same die were bonded onto a TO18 metal case and contacted by aluminium wires in order to reduce contact resistance.

3. Experimental results

The experimental steady-state J-V characteristics, at different operating temperatures were measured with a HP4155 Semiconductor Parameter Analyser. All the devices showed good rectifying

characteristics in the 298-523 K temperature range. The forward *J-V* curves are shown in Fig. 2, where the calculated slope for the ideality factor n = 1 and n = 2 are also drew for reference. The maximum temperature of 523 K was limited by the PID controlled oven. To avoid excessive heating of the aluminium wires employed for bonding, a compliance current of 380 mA was set in the HP4155 for all measurements. The static forward voltage drop at this current level was found close to 5 V at T = 298 K and, as expected, the same decreases with increasing temperatures. It should be noted that at room temperature an ideality factor always lower than 2 can be observed before current injection become significant, approximately for a bias voltage V_d > 2.7 V. This voltage decreases to 2.3 V for T = 523 K. An ideality factor close to 2 can be observed only at the highest temperatures and this should be a proof of an efficient post-implantation 4H-SiC crystal recovery. At room temperature, for which the curve down bending starts at around V_d = 2.9 V with a current density of about 20 A/cm^2, a diode differential resistance of 4.4 mΩ·cm^2 was calculated.

In reverse bias conditions the leakage current was found to be less than 0.2 nA at -100 V and T = 298 K. The breakdown voltage occurs at about -1 kV, in accordance with the theoretical limit calculated for a critical electric field of 2.2 MV/cm in the n-type epilayer film. This value was derived by the empirical relationship given by [20], which shows the dependence of breakdown field strength with drift region doping in 4H-SiC devices.

The turn-off switching characteristics of the diodes under study were also investigated in the 298-523 K temperature range. The diode was inserted into a test circuit, composed of a pulse generator and 60 Ω load resistor put in series with the device under test. The current was monitored by reading the voltage drop across the load resistor. The diode was switched from an initial on-state forward current I_F of about 60 mA to a reverse bias voltage of -10 V (instrument pulse amplitude limit). Typical reverse recovery current behaviours, measured at different temperatures, are shown in Fig. 3. The turn-off *di/dt* was about 1 A/µs. This transient analysis was characterized by measuring the peak reverse recovery current I_R and the reverse recovery time t_{rr}, defined as the interval between the time when the current crosses the zero value and the time when the current reaches the 25% of the I_R value [21]. The switching performance exhibits low dynamic losses and it is impossible to detect a significant storage time, namely a time interval related to a constant reverse current phase. I_R increases from 13 mA at room temperature, up to 27 mA at T = 523 K, with an I_F/I_R ratio of 4.5 and 2.5

respectively. A maximum reverse recovery time as short as 80 ns was measured for all samples over the whole range of test conditions, with a rather limited temperature dependence in the order of 10%.

As well known, during the diode turn-off, a carrier excess in the drift layer (holes and electrons injected from the anode and cathode region respectively) has to be removed by carrier sweep-out and recombination. Therefore, the minority carrier lifetime in the accumulation region is an important material parameter determining the switching operation mode. In the SiC implanted structures, in addition to material native defects, depending on the fabrication process, an excess concentration of recombination centers is in particular expected near the metallurgical boundary of a p/n junction [11]. The effective minority carrier lifetime in the n^- region at room temperature was estimated from the diode turn-off switching experimental data as suggest in Ref [19], to be 15 ns. The total reverse recovery charge was also calculated, resulting about 0.9 nC with a corresponding average carrier density, in the n^- region, close to 1.2×10^{16} cm^{-3}. This concentration, considering the n-type epilayer doping, is a proof of an appreciable resistance modulation effect in the n^- region, even at relatively small current levels.

Finally, the transient analysis of the investigated 4H-SiC diodes was compared to that of a commercially available high-speed switching silicon epitaxial planar diode (1N4148), with quite similar continuous forward current characteristics. The diodes turn-off performance comparison, under the same previously described electrical operation conditions, at T = 298 and 431 K, is illustrated in Fig. 4. Even though the 1N4148 is designed and optimised to be a fast switching device, the presented 4H-SiC p-i-n diode exhibits a transient performance practically comparable. In details, the Si switching losses are generally a bit less (I_R = 10 mA at room temperature), but as the temperature increases the difference between the Si and 4H-SiC peak reverse recovery currents decreases. On the other hand, T = 431 K is a value close to the 1N4148 maximum operating temperature range limit [22] while, as shown, the 4H-SiC diode virtually continues to work fine also for a much higher temperature regime.

4. Simulation analysis

Using the ATLAS physics based device simulator to study the DC characteristics of these 4H-SiC p-i-n diodes, a specific set of physical models, tuned and tested by comparison to experimental results,

was already presented in Ref. [17]. A good data agreement was achieved at different temperatures in the whole explored current range. The role of electrons and holes current components was analysed and some design considerations, on the anode doping electrically effective profile shape, were made. In this work, the same simulation structure was used, considering the equivalent lumped test circuit, to investigate the diode turn-off switching behaviours and to validate the developed numerical analysis. The fundamental 4H-SiC and model parameters assumed at room temperature are summarized in Table 1 [2, 23-25] with E_g bandgap energy, v_s saturated velocity, n_i intrinsic concentration, ε dielectric constant, E_A and E_D acceptor and donor energy levels, $\tau_{base\ p,n}$ effective carrier lifetimes in the n^- region, $C_{n,p}$ Auger recombination coefficients, $\mu_{max\ n,p}$ and $\mu_{min\ n,p}$ carrier mobilities for the Caughey-Thomas analytic model, and $N_{crit\ n,p}$ doping concentration at which the mobility is halfway between the min. and max. value. From Table 1, computing the ambipolar diffusion coefficient and then the ambipolar diffusion length L_a, the long diode condition $W/L_a > 2$, where W is the drift layer width, is verified [19]. Furthermore the calculated theoretical ohmic resistance of the non-modulated epilayer film is 5 m$\Omega\cdot$cm^2.

The carrier distribution across the diode during the switch-on state condition at room temperature, corresponding to a current density J_F of about 62 A/cm^2 and a voltage bias close to 3.5 V, is illustrated in Fig. 5. Starting from the anode surface, where the hole concentration is about 3×10^{17} cm^{-3}, the real hole concentration in the anode region, calculated by the simulator taking into account the incomplete ionization of Al atoms, is shown. In fact, in an Al implanted 4H-SiC region, at high doping levels, only a fraction of the implanted Al atoms, that really occupy a substitutional position in the crystal structure, gives origin to free holes [13]. Looking at the hole and electron concentrations in the drift layer, as discussed in Ref. [17], this forward bias establishes the beginning of the high injection regime.

The simulated and experimental diode turn-off switching waveforms at four distinct temperatures are shown in Fig. 6. The simulated results fairly mach the experimental data in terms of peak reverse recovery current and stored charge density. The differences in the reverse current tails are to be related to parasitic electrical effects in the measurement setup, occurring after the diode turn-off.

The carrier concentration decay at room temperature and in different moments of the transient analysis, namely $t_{1\text{-}5}$, is reported in Fig. 7. The inset schematizes the correspondence in the current

curve of these time instants: t_1 represents the initial switching on-state condition of the diode current density, t_2 is the zero crossing instant, t_3 is the time when the peak reverse recovery current appears, t_4 is the point in the reverse recovery current phase where $J = J_R/2$, and t_5 is at $J_R/4$. When the turn-off switching starts, the current recovery waveform is associated to a progressive removal of the excess charge at the extremities of the drift region, in particular at the anode interface. Here the carrier concentrations decay rapidly during the recovery transient and in t_3, where the peak reverse current appears, the excess charge related to the background doping is already significantly reduced. This is an explicit effect of both the carriers sweep-out, dues to the expanding of the depletion region to support the applied reverse bias, and the carrier recombination. Finally, considering the low carrier lifetimes, starting from t_5, the remaining charge in the quasi-neutral drift region implies a very limited recovery current tail. Increasing the temperature in the range of test conditions, the electron and hole concentrations across the diode increase less than one order of magnitude and an additional little excess of charge needs to be removed during the turn-off switching, explaining the limited temperature dependence of the reverse recovery time.

5. Conclusions

This paper has presented the steady-state and turn-off switching behaviour of Al implanted 4H-SiC p-i-n diodes in the 298-523 K temperature range. All the devices have shown good rectifying *J-V* characteristics and at room temperature the experimental forward current density was found close to 370 A/cm^2 at 5 V. The transient analysis of the diodes has shown the potential of bipolar SiC devices in fast switching applications, especially at high temperature. The commercial 1N4148 high-speed switching Si diode was also investigated for comparison under the same electrical operation conditions. A turn-off recovery time lower than 80 ns was measured for the 4H-SiC diodes in the whole range of test conditions. By means of a physics based device simulator this switching performance was related to a combination of low carrier lifetime and low excess charge in the drift region.

Acknowledgments

The authors would like to thank the staffs of the clean rooms and of the ion beams departments of

CNR-IMM in Bologna Italy, for the manufacture of the 4H-SiC diodes, and Department of Physics of the University of Padova Italy, for the SIMS analyses of the devices.

References

[1] Berger LI. Semiconductor Materials. New York: CRC Press; 1997.

[2] Harris GL. Properties of SiC. London: Institute of Electrical Engineers; 1995.

[3] Cooper JA, Agarwal A. SiC power-switching devices-The second electronics revolution?. Proc. IEEE 2002; 90:956–68.

[4] Wang J, Williams BW. Evaluation of high-voltage 4H-SiC switching devices. IEEE Trans. Electron Devices 1999; 46:589-97.

[5] Elford A, Mawby PA. The numerical modelling of silicon carbide high power semiconductor devices. Microelectronics Journal 1999; 30:527-34.

[6] Weitzel CE, Palmour JW, Carter Jr CH, Moore K, Nordquist KJ, Allen S, et al. Silicon carbide high-power devices. IEEE Trans. Electron Devices 1996; 43:1732-40.

[7] Palmour JW, Singh R, Glass RC, Kordina O, Carter Jr CH. Silicon carbide for power devices. Proc. 9th Int. Symp. Power Semiconductor Devices and IC's 1997; 1:25-35.

[8] Choyke WJ, Matsunami H, Pensl G. Silicon Carbide – Recent Major Advances. Berlin: Springer; 2003.

[9] Powell AR, Rowland LB. SiC materials – progress, status and potential roadblocks. Proc. IEEE 2002; 90:942-955.

[10] Badila M, Brezeanu G, Dilimot G, Millan J, Godignon P, Chante JP, et al. An improved technology of 6H-SiC power diodes. Microelectronics Journal 2000; 31:955-62.

[11] Feng ZC, Zhao JH. Silicon Carbide: Materials, Processing and Devices. New York: Taylor & Francis; 2004.

[12] Godignon P, Morvan E, Jordà X, Vellvehi M, Flores D, Rebollo J. SiC power DIMOS with double implanted Al/B P-well. Microelectronics Journal 2001; 32:503-7.

[13] Lades M, Kaindl W, Kaminski N, Niemann E, Wachutka G. Dynamics of Incomplete Ionized Dopants and Their Impact on 4H/6H-SiC Devices. IEEE Trans. Electron Devices 1999; 46:598-604.

[14] Rao MV. Maturing ion-implantation technology and its device applications in SiC. Solid State Electron. 2003; 47:213-222.

[15] Capano MA, Ryu S, Cooper Jr JA, Melloch MR, Rottner K, Karlsson S, et al. Surface roughening in ion implanted 4H-Silicon Carbide. J. Electronics Materials. 1999; 28:214-8.

[16] Silvaco International. ATLAS User Manual. Santa Clara: CA; 2006.

[17] Della Corte FG, Pezzimenti F, Nipoti R. Simulation and experimental results on the forward J-V characteristic of Al implanted 4H-SiC p-i-n diodes. Microelectronics Journal 2007; 38:1273-9.

[18] Poggi A, Bergamini F, Nipoti R, Solmi S, Carnera A. Effects of heating ramp rates on the characteristics of Al implanted 4H-SiC junctions. Appl. Phys. Lett. 2006; 88:162106-9.

[19] Sze SM. Physics of Semiconductor Devices. New York: Wiley-Interscience; 1981; ch.2.

[20] Singh R, Cooper JA, Melloch MR, Chow TP, Palmour JW. SiC Power Schottky and PiN Diodes. IEEE Trans. Electron Devices 2002; 49:665-72.

[21] Baliga BJ. Power Semiconductor Devices. Boston: MA-PWS; 1996.

[22] General Semiconductor 1N4148 datasheet.

[23] Ayalew T, Grasser T, Kosinam H, Selberherr S. Modeling of Lattice Site-Dependent Incomplete Ionozation in α-SiC Devices. Materials Science Forum 2005; 483:845-8.

[24] Levinshtein ME, Mnatsakanov T, Ivanov P, Palmour JW, Rumyantsev SL, Singh R, et al. “Paradoxes” of Carrier Lifetime Measurements in High-Voltage SiC Diodes. IEEE Trans. Electron Devices 2001; 48:1703-10.

[25] Galeckas A, Linnros J, Grivickas V, Lindefelf U, Hallin C. Auger recombination in 4H-SiC: Unusual temperature behaviour. Appl. Phys. Lett. 1997; 71:3269-71.

Figure captions

Fig. 1. SIMS profile of the aluminium implanted doping concentration.

Fig. 2. Measured forward *J*-*V* characteristics at different temperatures. The calculated slope for $n = 1$ and $n = 2$ are also traced for reference.

Fig. 3. Typical reverse recovery current waveform of the investigated 4H-SiC p-i-n diodes, measured at different temperatures.

Fig. 4. Reverse recovery characteristic comparison between the investigated 4H-SiC and the commercial 1N4148 Si diodes, at two different temperatures.

Fig. 5. Electron and hole distribution across the diode during the on-state switching condition ($J_F \approx 62$ A/cm^2, $V_d \approx 3.5$ V) at $T = 298$ K. The net doping level in the n^- region is also shown for reference.

Fig. 6. Simulated and experimental (symbols) turn-off behaviour at four distinct temperatures for the analysed 4H-SiC p-i-n diode.

Fig. 7. Electron and hole concentration decay in different time instants of the transient analysis. $T = 298$ K.

Tables

Table 1: Simulation model parameters assumed at room temperature. Other parameters were set as in [17].

E_g (eV)	3.2
v_s (cm^2/s)	2×10^7
n_i (cm^{-3})	1.99×10^{-8}
ε	9.66
E_A (eV)	0.19
E_D (eV)	0.05
$\tau_{\mathrm{base\ p,n}}$ (ns)	15
$C_{n,p}$ (cm^6/s)	5×10^{-31} , 2×10^{-31}
$\mu_{\mathrm{max\ n,p}}$ (cm^2/V·s)	200 , 20
$\mu_{\mathrm{min\ n,p}}$ (cm^2/V·s)	6 , 2
$N_{\mathrm{crit\ n,p}}$ (cm^{-3})	1×10^{16}

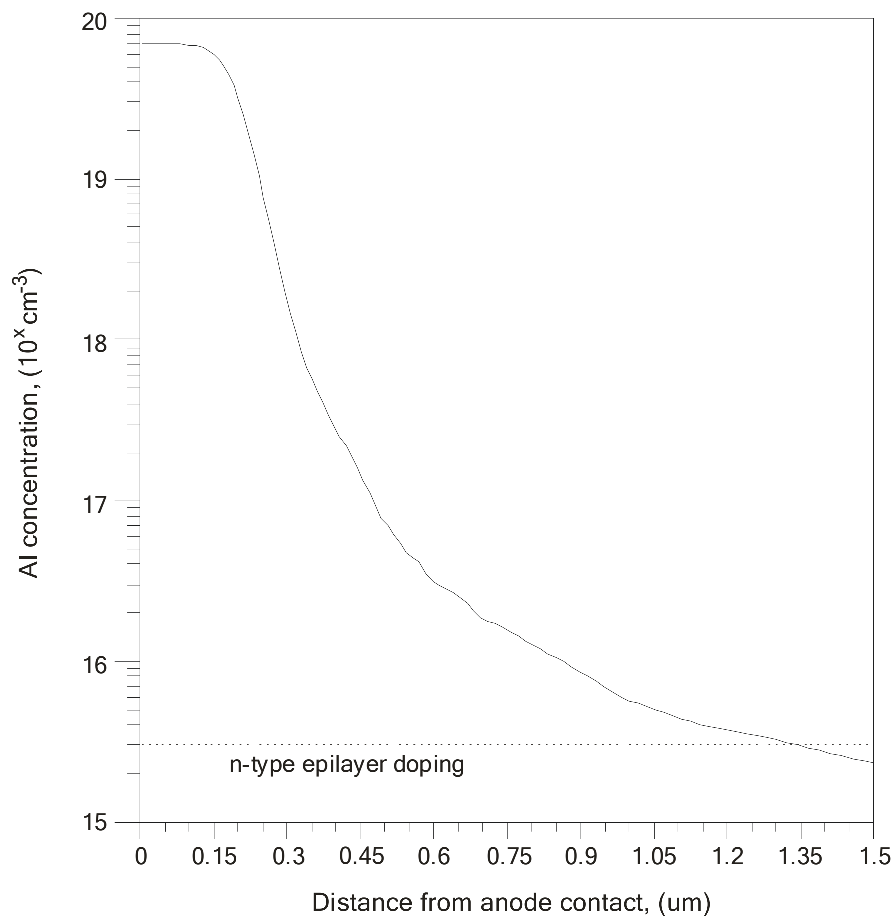

Figure 1

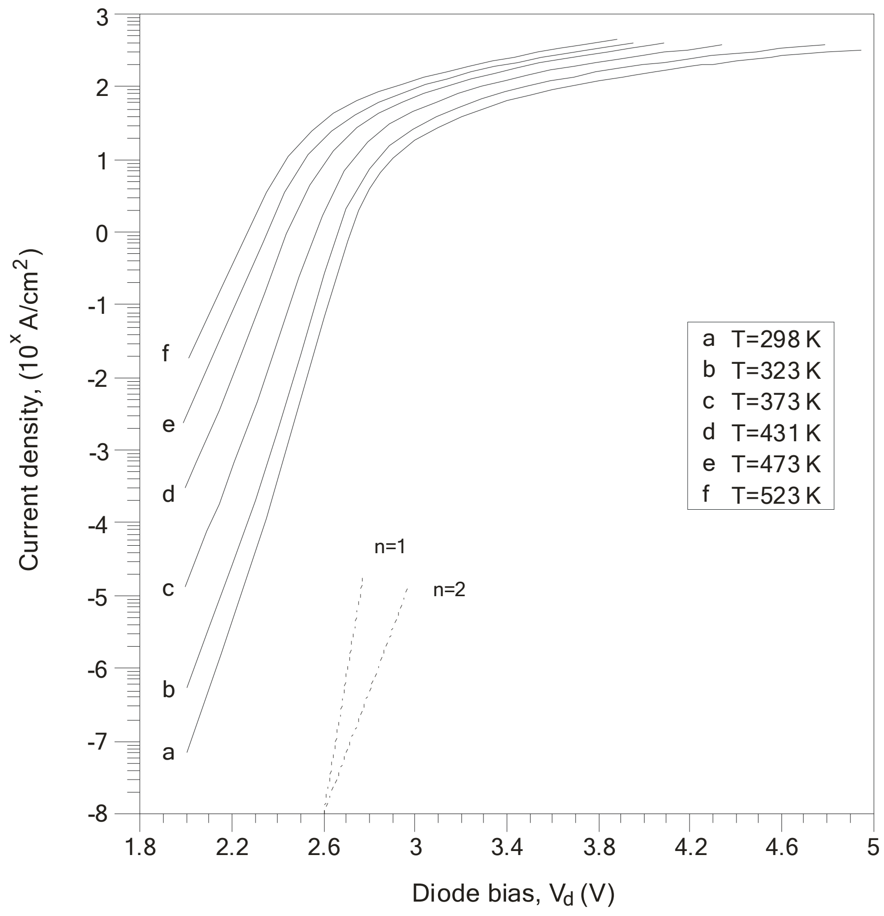

Figure 2

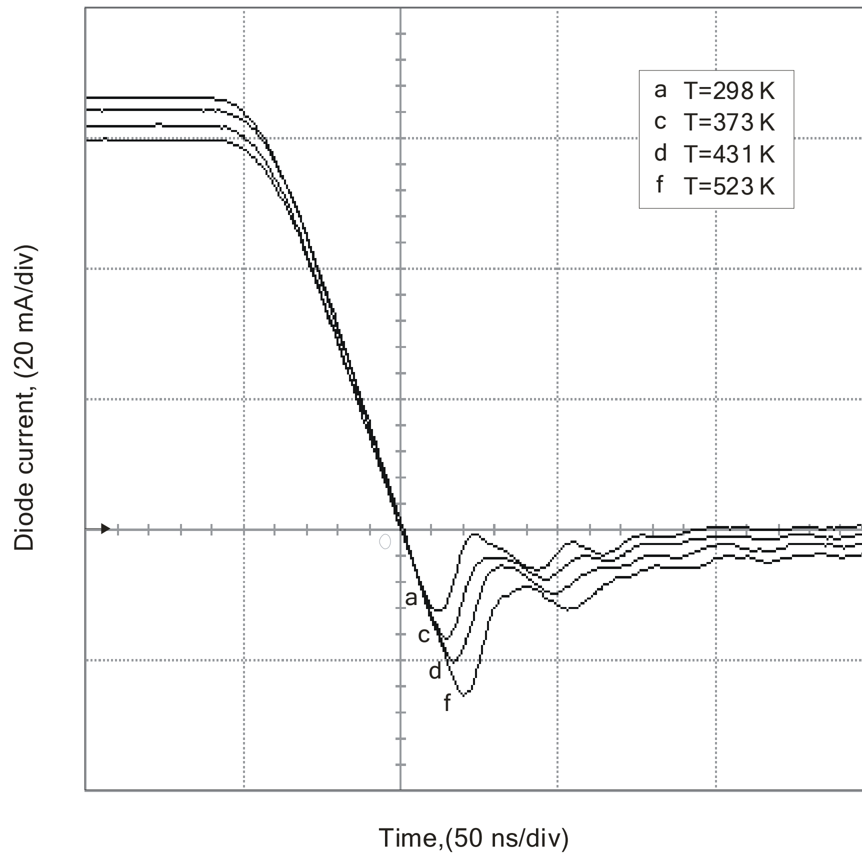

Figure 3

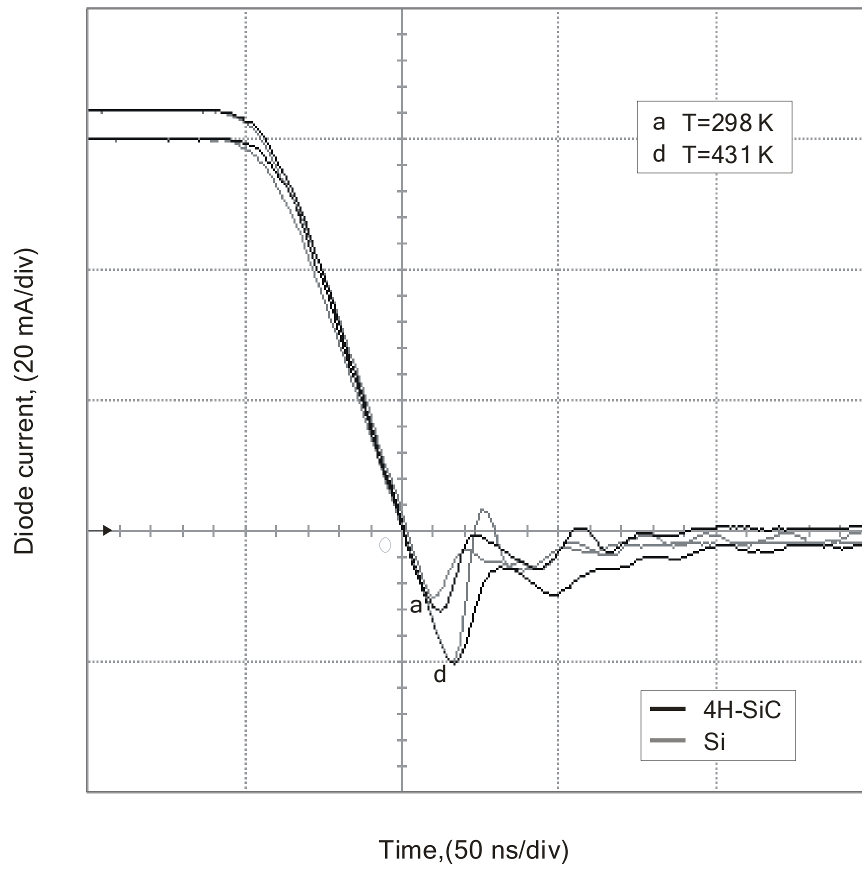

Figure 4

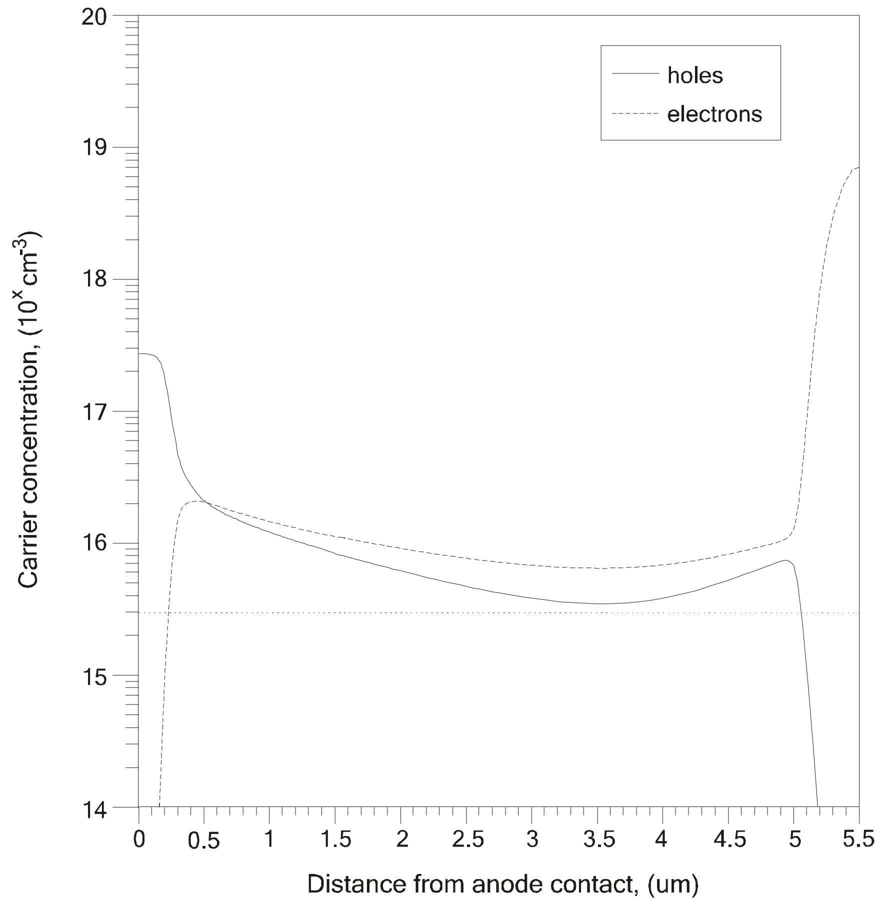

Figure 5

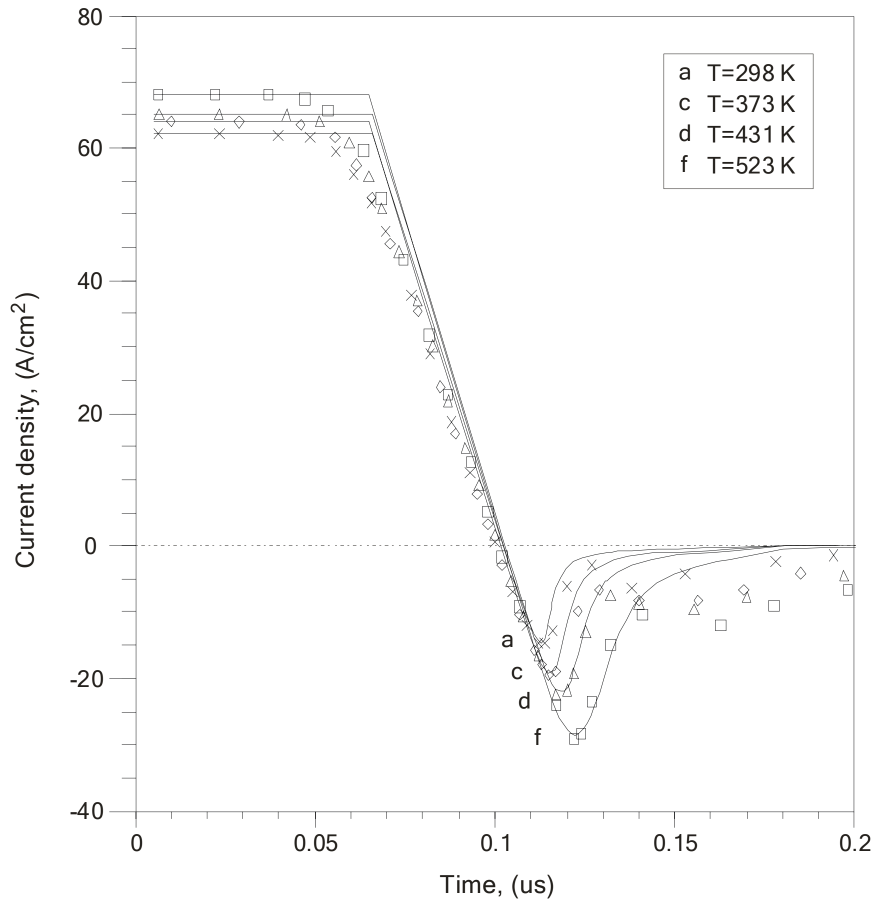

Figure 6

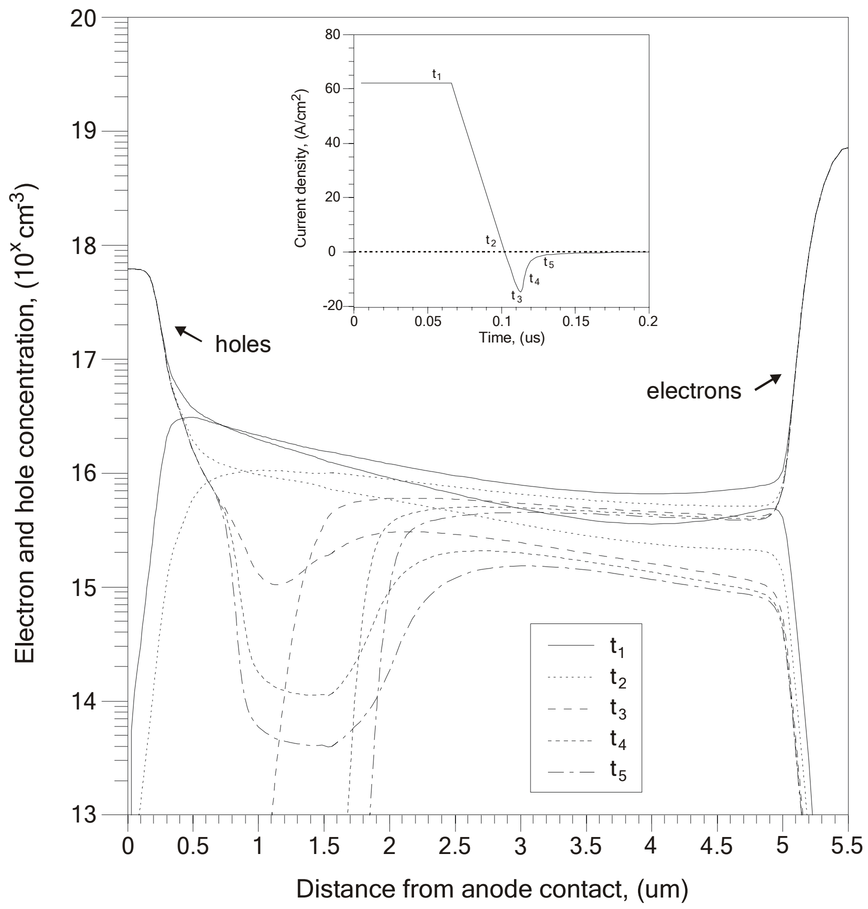

Figure 7